PHYSICAL REVIEW A VOLUME 23, NUMBER 1 JANUARY 1981

Theoretical study of near-resonant charge-exchange collisions of H^+ with alkali atoms

C. Kubach and V. Sidis*

Laboratoire des Collisions Atomiques et Moléculaires; Bâtiment 351, Université Paris-Sud, 91405 Orsay Cedex, France

(Received 19 March 1980)

Our earlier study of the H^+-Cs collision is extended to the lighter H^+–alkali-atom systems. The previous one-electron projected-valence-bond approximation is further simplified and improved by the use of an effective screened Coulomb potential to represent the alkali$^+$ core. This method is found to reproduce very accurately the results of a complete all-electron calculation performed on the $(Li\text{-}H)^+$ system. Total cross sections for charge exchange into $H(n = 2) + \text{alkali}^+$ are obtained from diabatic 7-state close-coupling calculations. The theoretical results nicely agree with the available experimental data for the H^+-K and -Rb systems. On the other hand, the calculated cross section for H^+-Na is significantly smaller than the experimental results; possible sources of this discrepancy are discussed.

I. INTRODUCTION

A number of measurements have been performed on charge-exchange collisions of protons with alkali atoms in the medium energy range (few tens of eV to few keV. In these systems charge-exchange excitation is expected to be dominant since the reactions

$$H^+ + A \to H(n=2) + A^+ ,\quad (A = Cs,\ Rb,\ K,\ Na,\ Li), \tag{1}$$

are nearly resonant ($\Delta E = -0.49$ eV for Cs to $\Delta E = -1.99$ eV for Li) Accordingly, experiments were undertaken to study the efficiency of these reactions in the production of intense $H(2s)$ metastable beams. Owing to its particularly small resonance-energy defect the $H^+ + Cs$ system has been the most widely investigated,[1-5] while H^+ collisions with the lighter alkali atoms have been much less studied experimentally.[3-6]

On the theoretical side also the only thoroughly investigated H^+-alkali collision is to our knowledge $H^+ - Cs$ (Refs. 2, 7–9). However, adiabatic molecular properties of lighter (H-alkali)$^+$ systems have been published by Valance[10(a)] and by Olson *et al.*[10(b)] The latter calculations have enabled the theoretical prediction of low-energy elastic scattering of H^+ by K and Na. Only for the $(H\text{-}Na)^+$ collisional system have the relevant dynamic couplings been calculated,[11] but no inelastic cross-section results were reported. Generally molecular properties can be obtained using all-electron calculations involving large scale configuration interaction (CI) techniques.[10(b)] Nevertheless, it is tempting to represent the (H-alkali)$^+$ systems by a single active outer electron in the field of the two inert cores. This view suggests the use of one-electron effective potential methods. In this respect, Olson *et al.*[8] assumed that the core electrons completely screen the nuclear charge, whereas effective screening was accounted for in the Hellmann-type pseudopotential calculations of Valance.[1,10,11] The complete screening is valid provided the active electron remains always outside the alkaki$^+$ core. It was shown by Sidis and Kubach[9] that this condition is fulfilled down to relatively small internuclear distances R provided the active electron is described by suitably projected orbitals (see Fig. 1 in Ref. 9). To improve the accuracy of the previously proposed method[9] an alternative approach involving a screened Coulomb effective potential is introduced in Sec. II. Adiabatic potential energy curves for the considered (H-Rb, K, Na)$^+$ systems are calculated for comparison with the available theoretical results.[10] For reasons developed in our previous studies of near-resonant charge-exchange collisions the cross-section calculations are performed in a *diabatic* projected-valence-bond (PVB) representation.[9] The results are presented and compared with the experimental data in Sec. III.

II. MOLECULAR ASPECT OF THE COLLISION PROBLEM

A. Model Hamiltonians and test calculations

In view of the occurrence of near-resonant charge-exchange transitions at relatively large internuclear distances R an essentially *atomic* description of the problem is most appropriate. Accordingly, we have chosen a projected-valence-bond (PVB) representation.[12] The procedure follows closely that described in ref. 9. Briefly, we start with a self-consistent field (SCF) calculation on the A^+ alkali core which generates both the inner (core) and the outer (valence and Rydberg) SCF orbitals of the considered alkaki atom. Then we consider many-electron wave functions $|A^+\phi\rangle$ representing single configurations built from all the frozen atomic SCF core orbitals (A^+) and an outer electron orbital (ϕ). In the H^+-$A^{(*)}$ channels, ϕ is the valence ns_A (or the first Rydberg np_A) SCF orbital. In the $\mathrm{H}^{(*)}$-A^+channels, ϕ is the exact $1s_{\mathrm{H}}$ $2s_{\mathrm{H}}$, $2p_{\mathrm{H}}$) hydrogen wave function orthogonalized to all the above alkali SCF orbitals. The matrix elements of the all-electron Hamiltonian H_{el} in such a PVB basis are easily seen to be those of the following one-electron Hamiltonian acting on the outer orbital

$$\mathcal{H} = \left(E_A{}^+ - 2 \sum_{j \in A^+} \langle j \,|\frac{1}{r_{\mathrm{H}}}\,| j \rangle\right) + P^0_A\left(F_A{}^+ - \frac{1}{r_{\mathrm{H}}}\right) P^0_A$$
$$+ P^0_{\tilde{\mathrm{H}}}\left(F_A{}^+ - \frac{1}{r_{\mathrm{H}}}\right) P^0_{\tilde{\mathrm{H}}} . \qquad (2)$$

In Eq. (2), P^0_A is the projector onto the space spanned by the selected outer (valence, Rydberg) orbitals $|\phi_A\rangle$ of the alakli atom and $P^0_{\tilde{\mathrm{H}}}$ the projector onto the space spanned by the H orbitals $|\phi_{\tilde{\mathrm{H}}}\rangle$ orthogonalized to the core and outer alkali orbitals. $F_A{}^+$ is the closed-shell Fock operator of the A^+ ground-state configuration and $E_A{}^+$ is the energy of the A^+ core which can be taken as an energy origin. The approximation made in Ref. 9 consisted of replacing the $F_A{}^+$ operator in the last term of Eq. (2) by $-\Delta/2 - 1/r_A$ arguing that the $|\phi_{\tilde{\mathrm{H}}}\rangle$ orbitals essentially describe the motion of an electron far from the alkali center. This approximation can be improved by adding to the $-1/r_A$ term an effective potential $V_A(r_A)$ accounting for the imcomplete screening of the alkaki nucleus when the electron described by $|\phi_{\tilde{\mathrm{H}}}\rangle$ penetrates inside the core boundary. The form chosen for $V_A(r_A)$ is a screened Coulomb potential:

$$V_A(r_A) = A \exp(-a r_A)/r_A . \qquad (3)$$

The parameters A and a (Table I) are determined by requiring the two matrix elements,

$$\left\langle ns_A(np_A) \;\middle|\; -\frac{1}{2}\Delta - \frac{1}{r_A} + V_A(r_A) \;\middle|\; ns_A(np_A)\right\rangle ,$$

($n=2$, 3, 4, 5, and 6 for $A=$ Li, Na, K, Rb, and Cs, respectively) to reproduce the corresponding eigenvalues of the Fock opperator $F_A{}^+$ (self-consistent field (SCF) energies of the valence ns_A and first Rydberg np_A orbitals). In view of the way the potential of Eq. (3) is determined and of the compactness of the A^+ core orbitals [enabling the replacement of $2\sum_{j\in A^+}\langle j\,|1/r_{\mathrm{H}}|\,j\rangle$ in Eq. (2) by $(Z_A - 1)/R$] it was tempting to proceed to a further simplification of the above effective Hamiltonian to the form

$$\mathcal{H} \approx E_A{}^+ + (P^0_A + P^0_{\tilde{\mathrm{H}}})\left(-\frac{1}{2}\Delta - \frac{1}{r_{\mathrm{H}}} - \frac{1}{r_A} + V_A(r_A)\right)$$
$$\times (P^0_A + P^0_{\tilde{\mathrm{H}}}) + \frac{1}{R} . \qquad (4)$$

TABLE I. Parameters (A, a) of the effective potential [Eq. (3)] for the alkali atoms.

	A (a.u.)	a (a_0^{-1})
Li	2.23	2.774
Na	10.00	2.492
K	19.53	2.44
Rb	33.74	2.34
Cs	49.75	1.775

Calculations involving the one-electron model Hamiltonian of Eq. (4) with and without[9] the $V_A(r_A)$ term have been performed for (Li-H)$^+$ and compared with the all-electron PVB results (i.e., matrix elements of the actual all-electron Hamiltonian H_{el} in the defined PVB basis $|A^+\phi\rangle$). The considered PVB orbital basis consisted of

$$1s_{\mathrm{Li}},\quad 2s_{\mathrm{Li}},\quad 2p_{\mathrm{Li}},\quad 1s_{\mathrm{H}},\quad 2s_{\mathrm{H}},\quad 2p_{\mathrm{H}} .$$

The expansion Slater orbital (STO) basis set used for Li is taken from Krauss *et al.*[13] (the binding energies of $2s_{\mathrm{Li}}$ and $2p_{\mathrm{Li}}$ agree with experiment[14] within 4.10^{-2} eV). The calculation involving the model Hamiltonian of Eq. (4) reproduces the all-electron results to better than 5.10^{-3} eV for $R \geqslant 5a_0$. As additional information a similar two-center potential used in the (He-Na)$^+$ case[15] yielded equally good agreement with the corresponding all-electron PVB calculation. It can thus be claimed that (for a given STO basis set and for the charge-exchange problems under consideration) *the model PVB calculation [Eq. (4)] yields as accurate results as all-electron calculations at large and moderate internuclear distances* ($R \geqslant 5a_0$).

Comparing the results of the model Hamiltonians Eq. (4) obtained with or without the inclusion of $V_A(r_A)$, it is found that the deviations remain generally small (Figs. 1 and 2) confirming our presuppositions.[9] Note that in all the above calculations (as well as in all the calculations reported in Sec. II B) we have used the hybrid $\tilde{\phi}^{\pm}_{\mathrm{H}} = (2\tilde{s}_{\mathrm{H}} \pm 2\tilde{p}_{\mathrm{H}})/\sqrt{2}$ projected orbitals which are most appropriate to the simultaneous treatment of exchange and polarization [linear Stark effect for $H(n=2)$].[2,9,16] Inspection of Fig. 1 reveals that the deviations ($\leqslant 1.5\times10^{-3}$ a.u.) showing up with decreasing R in the $\mathrm{Li}^+\,\tilde{\phi}^+_{\mathrm{H}}$ energy curve do not appear in the $\mathrm{Li}^+\,\tilde{\phi}^-_{\mathrm{H}}$ curve. This is readily understood recalling that the $\tilde{\phi}^-_{\mathrm{H}}$ orbital which is not oriented towards the Li^+ center penetrates much less the Li^+ core than $\tilde{\phi}^+_{\mathrm{H}}$. In Fig. 2 are compared the results of the model and all-electron calculations for the potential well in the

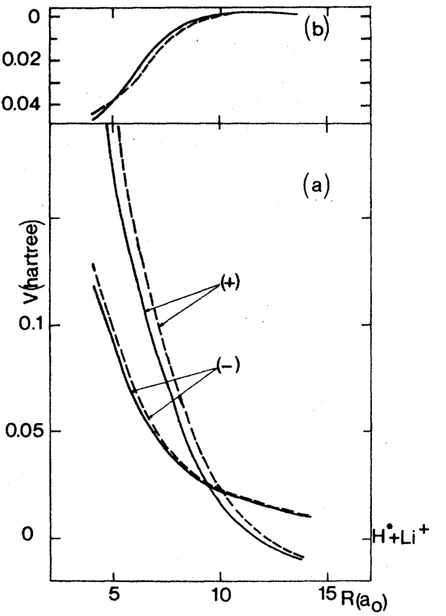

FIG. 1. Results of PVB calculations on the (H-Li)$^+$ system. Dashed lines: model one-electron Hamiltonian of Eq. (4) in text without the V_A (r_A) term, full lines: all-electron and model one-electron Hamiltonian of Eq. (4) in text (these two calculations are indistinguishable to the scale of the figure). (a) Potential energy curves of the diabatic PVB states correlated with Li$^+$ + H*[$\phi^{\pm} = (2s \pm 2p)/\sqrt{2}$]. (b) Electronic coupling between the ϕ^+ and ϕ^- diabatic PVB states.

energy curve correlated with H$^+$ + Li (2s). All the PVB-CI energy curves obtained by diagonalizing the $\mathcal{H}$ matrix in the 5-fold PVB subspace, Li$^+$ +H(1s), Li(2s) + H$^+$, Li*(2p) + H$^+$, Li$^+$ +H(2s, 2p), agree quite nicely. The SCF-CI curves shown in Fig. 2 are obtained by diagonalizing the H_{el} matrix in the space spanned by the SCF ground state [correlated with Li$^+$ + H(1s)] and states generated by single excitations to the corresponding lowest five virtual orbitals. It is noted that such an SCF-CI approach requires more states than the PVB-CI method to yield a correct potential well. This proves that the *PVB method accounts more easily for the exchange and polarization interactions of importance in the description of the adiabatic well.* (The difference between the 11-state SCF-CI calculation and the 5-state PVB-CI one is 10^{-3} a.u. at equilibrium distance. This gap can of course be removed by adding Rydberg or polarization orbitals to the PVB basis.) In concluding this section, it is worth pointing out that the present method [Eq. (4)] should not be confused with the Hellmann pseudopotential method[17] which generates the *nodeless orbital* reproducing the actual binding energy of the alkali atom.

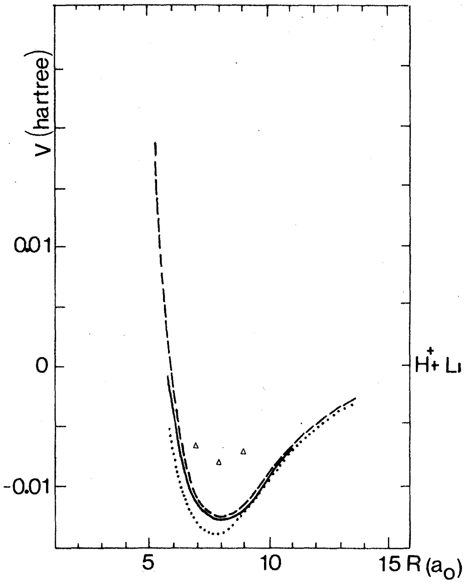

FIG. 2. Adiabatic potential energy curve correlated with H$^+$ + Li (2^{2}S). PVB-CI *calculations* (5-state CI); dashed lines: model one-electron Hamiltonian of Eq. (4) without the V_A (r_A) term; full line: all-electron and model one-electron Hamiltonian of Eq. (4) in text (these two calculations are indistinguishable to the scale of the figure). SCF-CI *calculations;* open triangles: 5-state CI; dotted line: 11-state CI.

B. Results

Model one-electron PVB calculations [Eq. (4)] have been carried out for (H-Cs, Rb, K, Na)$^+$. The alkali STO expansion basis for Cs is identical to that used in Ref. 9. For Rb the single-zeta STO basis: 1s to 4p of Clementi *et al.*[18(a)] has been used to expand the core orbitals. This set was augmented by four STO 5s, 5s', 5p, and 5p' with exponents 1.26, 0.75, 1, and 0.6, respectively. For K we used the 11s/6p basis of Clementi[18(b)] augmented with two STO: 4p and 4p' with exponents 1 and 0.55, respectively. Finally the Na basis is that of Saxon et al.[18(c)] from which the d, f, and g STO have been deleted. The parameters A and a of the effective potential [Eqs. (3) and (4)] are given in Table I.

The method outlined in Sec. II A is completely *ab initio* since the determination of the effective potential depends exclusively on the *a priori* knowledge of SCF data. From Table II it is seen however, that the calculated SCF binding energies of the alkali atoms reproduce more or less satisfactorily the experimental data.[14,19] This discrepancy is either basis dependent or inherent to the Hartree-Fock approximation (i.e., lack of configuration interaction to account for core polarization[10(b)] or relativistic effects in

TABLE II. Comparison between the theoretical (T) and experimental (E) binding energies (ns, np; $n=2$, 3, 4, 5, 6 for Li, Na, K, Rb, Cs, respectively) and energy differences ($\Delta_{s\text{-}p}$), in atomic units, for the considered s, p orbitals of alkali atoms.

	Li		Na		K		Rb		Cs	
	T	E	T	E	T	E	T	E	T	E
ns	0.196	0.198	0.182	0.189	0.147	0.159	0.133	0.153	0.137	0.143
np	0.129	0.130	0.109	0.112	0.095	0.100	0.090	0.095	0.083	0.091
$\Delta_{s\text{-}p}$	0.067	0.068	0.073	0.077	0.052	0.059	0.043	0.058	0.054	0.052

the cases of Rb and Cs). In order to avoid spuriously enhanced charge-exchange transitions (Sec. III) due to underestimated resonance-energy defects between the $H^+ + A(ns)$ and the $H(n=2) + A^+$ channels the diagonal PVB matrix elements were shifted to match the experimental asymptotes.

In Table III is given the calculated static dipole polarizability of the considered ground-state alkali atoms and the quadrupole moment of their first excited P state. It is found that the present calculations generally overestimate the actual dipole polarizabilities.[20] Such a feature has been noticed in previous work[10] and is inherent to the frozen-core approximation which generally tends to overestimate the diffuseness of the outer alkali orbitals. Further discussion of this effect on the charge-exchange cross sections will be given in Sec. III.

Adiabatic potential energy curves have been obtained by diagonalizing the PVB Hamiltonian matrix in the *same* space as that used for treating the charge-exchange collision problem (i.e., five lowest Σ states and two lowest Π states, see Sec. III). The calculated adiabatic energy curves for the (H-Na, K, Rb)$^+$ systems are shown in Figs. 3–5. (Ref. 21). These energy curves behave generally in the same way as in the previously studied (H-Cs)$^+$ case.[9] However, when going from Cs to Li one observes a gradual reduction of the potential well in the energy curve correlated with $H^+ + A(n^2S)$, Table IV. This effect is caused by the increase of the energy gap between the $H^+ + A(n^2S)$ and $H(n=2) + A^+$ levels together with the decrease of the corresponding exchange interaction as well as by the decrease of the alkali-atom polarizability. For the (H-Cs)$^+$ system, the present calculation yields a slightly deeper potential well than that previously reported by us.[9] This difference (2.10^{-3} a.u.) does not significantly affect the previously calculated rainbow structures at low energy.

TABLE III. Comparison between the calculated (α_{Theor}) and the experimental (α_{Expt}) static dipole polarizabilities of ground-state alkali atoms (see also Table VII in Ref. 10). The calculated quadrupole moment (β) of the first Rydberg P state is also displayed.

	Na	K	Rb	Cs
$\alpha_{\text{Theor}}(a_0^3)$	179	352	440	440
$\alpha_{\text{Expt}}(a_0^3)$	165	281	296	350
$(\sqrt{\alpha_{\text{Expt}}/\alpha_{\text{Theor}}})^{1/2}$	0.96	0.89	0.82	0.89
$\beta(a_0^2)$	18.0	23.3	26.8	33.0

The behavior of the adiabatic potential energy curves is generally understandable in terms of polarization and exchange interactions. A particularly illustrative example is provided by the $\Sigma(\phi_{\text{H}}^+)$ energy curve correlated with $H(n=2) + A^+$. At large distance this curve behaves as $\sim -3/R^2$ (linear Stark effect) until a "cut-off distance" where the exchange interactions with the $\Sigma(ns_A, np_A)$ states correlated with $H^+ + A(ns, np)$ prevail. The increasing well in the $\Sigma(\phi_{\text{H}}^+)$ curve when going from Cs to Na is readily seen to result both from the decrease of the "cut-off distance" and from the decrease of the resonance-energy defect with respect to the $\Sigma(np_A)$ level.

All the calculated potential energy diagrams display the same avoided crossing pinching between the two Σ curves correlated with $H(n=2) + A^+$. This feature illustrates again the opposite effects

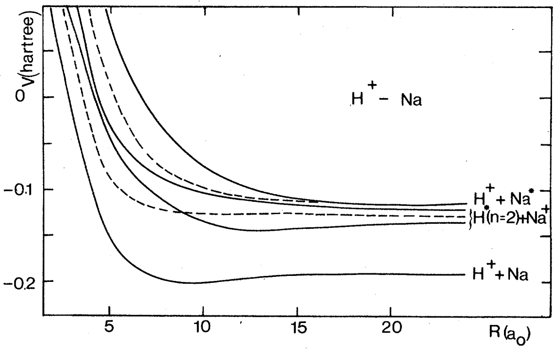

FIG. 3. Adiabatic one-electron PVB-CI potential energy curves for (H-Na)$^+$. Full lines: $^2\Sigma$ states; dashed lines: $^2\Pi$ states. Na and Na* stand, respectively, for Na(3^2S) and Na (3^2P).

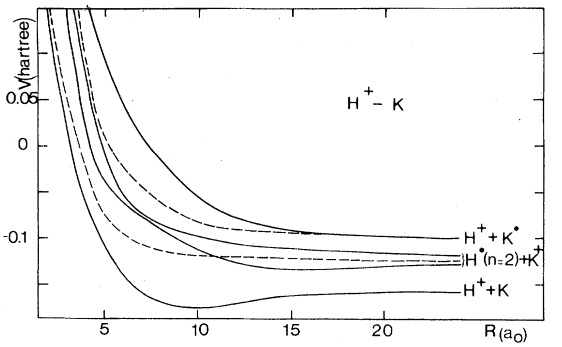

FIG. 4. Same caption as Fig. 3 except for $(\mathrm{H\text{-}K})^+$. K and K* stand, respectively, for $\mathrm{K}(4^2S)$ and $\mathrm{K}(4^2P)$.

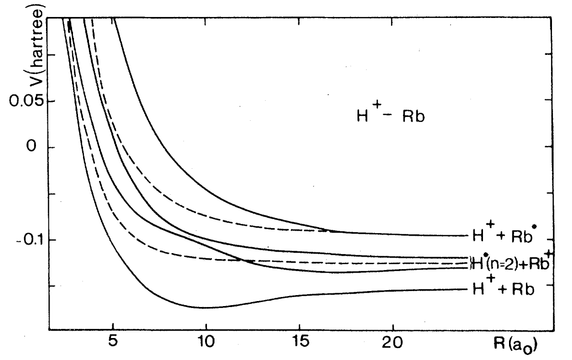

FIG. 5. Same caption as Fig. 3 except for $(\mathrm{H\text{-}Rb})^+$. Rb and Rb* stand, respectively, for Rb (5^2S) and $\mathrm{Rb}(5^2P)$.

of polarization (Stark effect) and promotion (exchange interaction) and is to be related to works concerned with diabatic molecular orbital (MO) correlations with L-shell atomic substates (see, e.g., Ref. 22).

It is interesting at this stage to compare the present results with previous adiabatic calculations.[10] Taking the large scale CI calculations of Olson *et al.*[10(b)] as a reference, it is found that both the present calculations and those of Valance[10(a)] underestimate the potential well depth and overestimate the equilibrium internuclear separation of the energy curve correlated with $\mathrm{H}^+ + A(\mathrm{ns})$. This defect is not so much a drawback of the frozen core one-electron model but it rather reflects the insufficient inclusion of higher Rydberg and/or polarization orbitals. This is well illustrated by results obtained on $(\mathrm{H\text{-}Cs})^+$ with different amounts of polarization orbitals (Table IV) and was discussed in detail in Ref. 12 (see also Fig. 2 and related comment in Sec. II A). This discussion implies that for the purpose of calculating *detailed elastic differential cross sections* for H^+/alkali collisions at low energy ($E \lesssim$ *few* eV), where the system behaves most adiabatically, our too restricted CI is insufficiently accurate and calculations of the type reported in Ref. 10(b) are recommended. However, for the inelastic processes of interest in the present work, the major concern should be the reliability of the interactions responsible for the corresponding electronic transitions. These interactions also directly determine the behavior of the adiabatic energy splittings between the molecular levels associated with the reactants and products. Since our calculations of these energy splittings (Table V) nicely agree with those resulting from the elaborate calculations of Olson *et al.*[10(b)] we are confident in the reliability of our molecular input data to the collisional cross-section calculations of Sec. III (we note that equally good agreement with the energy splittings of Valance[10(a)] is also found).

III. CROSS-SECTION CALCULATIONS

In all cases we have used a 7-state diabatic PVB expansion

$$|A^+\sigma ns_A\rangle\,,$$

$$|A^+\sigma 1\tilde{s}_{\mathrm{H}}\rangle\,,\quad |A^+\sigma\tilde{\phi}^+_{\mathrm{H}}\rangle\,,\quad |A^+\sigma\tilde{\phi}^-_{\mathrm{H}}\rangle\,,\quad |A^+\pi 2\tilde{p}_{\mathrm{H}}\rangle\,,$$

$$|A^+\sigma np_A\rangle\,,\quad |A^+\pi np_A\rangle\,,$$

$$(A = \mathrm{Rb},\ \mathrm{K},\ \mathrm{Na})\,.$$

In view of the occurrence of the charge-exchange transitions at relatively large impact parameters (small scattering angle) the calculations were performed in the straight-line impact parameter

TABLE IV. Potential well depth (U) and equilibrium distance (R_e) of the adiabatic energy curve correlated with H^+ + alkali (n^2S).

	Na			K			Rb		Cs		
	Present	Ref. 10(a)	Ref. 10(b)	Present	Ref. 10(a)	Ref. 10(b)	Present	Ref. 10(a)	I[a]	II[b]	Ref. 10(a)
U(eV)	0.39	0.34	0.469	0.49	0.49	0.614	0.55	0.5	0.56	0.71	0.70
$R_e(a_0)$	8.7	8.2	7.98	9.4	8.6	8.74	10.4	8.8	9.7	10.4	9.0

[a] I: Present work involving the $6s_{\mathrm{Cs}}$ and $6p_{\mathrm{Cs}}$ outer orbitals (the core being implicit).

[b] II: Same as I with additional inclusion of $5d_{\mathrm{Cs}}$, $7s_{\mathrm{Cs}}$, and $4f_{\mathrm{Cs}}$.

TABLE V. Σ adiabatic energy curves (a.u.) of the states correlated with $H^*(\phi^+)+A^+$, $H^*(\phi^-)+A^+$, and $H+A^*(n^2P)$ referred to that correlated with $H^+ + A(n^2S)$.

	$H^*(\phi^+)+A^+$		$H^*(\phi^-)+A^+$		$H^+ + A^*(n^2P)$	
$R(a_0)$	Present	Ref. 10(b)	Present	Ref. 10(b)	Present	Ref. 10(b)
			(a) $(H-K)^+$			
∞	0.034 51	0.034 13			0.058 29	
40	0.032 59		0.036 34		0.059 04	
30	0.031 14	0.030 92	0.037 83	0.037 66	0.058 84	0.059 17
25	0.029 73	0.029 25	0.039 38	0.039 12	0.058 76	0.057 93
22.5	0.028 66		0.040 62		0.058 97	
20	0.027 26	0.026 15	0.042 47	0.042 11	0.059 98	0.057 52
17.5	0.026 07		0.045 57		0.063 38	
15	0.028 16	0.025 73	0.051 52	0.050 69	0.072 39	0.068 70
12.5	0.038 99		0.062 33		0.091 38	
10	0.060 15	0.057 68	0.076 59	0.077 84	0.122 89	1.120 86
9	0.070 36	0.068 30	0.081 81	0.084 37	0.138 80	0.137 16
7.5	0.084 02	0.082 47	0.087 25	0.091 48	0.164 27	0.152 33
5	0.070 79	0.070 66	0.102 65	0.097 67	0.217 75	0.144 74
2.5	0.067 45		0.137 84		0.285 00	
			(b) $(H-Na)^+$			
40	0.061 85		0.065 61		0.076 96	
30	0.060 34	0.060 60	0.067 03	0.067 36	0.076 78	0.077 55
25	0.058 81	0.058 75	0.068 45	0.068 75	0.076 63	0.076 93
22.5	0.057 61		0.069 57		0.076 61	
20	0.055 85	0.055 17	0.071 15	0.071 40	0.076 96	0.076 31
17.5	0.053 17		0.073 55		0.078 67	
15	0.050 11	0.048 67	0.077 53	0.077 65	0.084 11	0.084 30
12.5	0.050 79		0.084 97		0.097 62	
10	0.063 79	0.063 56	0.098 39	0.099 30	0.125 85	0.126 80
7.5	0.091 80	0.092 87	0.115 10	0.117 94	0.174 01	0.171 49
5	0.114 38	0.112 27	0.119 30	0.124 62	0.229 00	0.196 59
2.5	0.089 64	0.092 34	0.152 22	0.149 58	0.256 07	0.202 74

[a] For $(H-Na)^+$ comparison is made after a 2.94×10^{-3} a.u. downward shift of the $A^2\Sigma^+$ curve of Ref. 10(b) in order that this curve matches the actual $H^+ + Na(3^2S)$ asymptotic limit.

approximation.[23]

Calculation of the relative fraction of metastable H (2*s*) and radiating H (2*p*) states, which can be achieved along the lines of our previous work,[9] has not been attempted here. The reason being simply that this sharing process is mainly governed by the long-range interactions (Stark effect and rotational coupling) between the $\sigma\tilde{2}s_H$, $\sigma\tilde{2}p_H$, and $\pi2\tilde{p}_H$ states and it is therefore expected to be quite similar in all the H$^+$ alkali systems. This prediction is indeed qualitatively confirmed by the experimental results of Nagata.[5(a)]

Before undertaking the systematic calculation of the cross sections we wondered whether the results might be sensitive to our overestimation of the alkali-atom dipole polarizabilities (Table III). To investigate this effect we have multiplied the $\langle ns_A|\mathcal{H}(\text{Eq. 4})|np_A\rangle$ PVB matrix elements by the factor $(\alpha_{\text{Exp}}/\alpha_{Th})^{1/2}$ of Table III. This readjustment is based on second-order perturbation theory where the alkali-atom polarizability is essentially proportional to the square of the ns_A-np_A interaction [see, e.g., Eq. (1) in Ref. 15]. It turned out that neither the comparison of the energy splittings of Table V nor the cross-section results were significantly affected by this correction (10% variation at most). All the results reported below take these corrected dipole polarizabilities into account.

The calculated total charge-exchange cross sections are shown in Figs. 6–8. For H$^+$-Rb and -K the available experiments[3-6] mutually agree and the present calculations quite nicely reproduce the results of Nagata.[5(b)] Also presented in Figs. 6 and 7 are the excitation cross sections Q_{4p_K} and $Q_{5p_{Rb}}$ which are intended to roughly represent the rise of other inelastic processes than charge exchange into H($n=2$). The general trend of these cross sections is similar to the corresponding $Q_{6p_{Cs}}$ one in the H$^+$-Cs system.[9] These results stress the importance of using a multistate expansion in the treatment of near-resonant

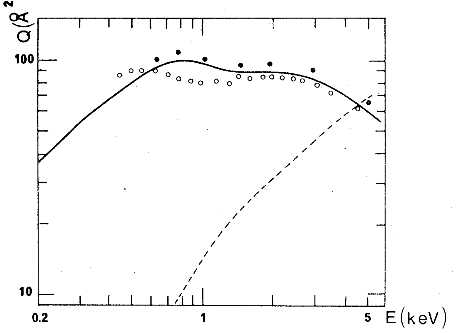

FIG. 6. Total summed $Q_{(2s+2p)_H}$ charge-exchange cross section for the H^+-Rb collision; full line: present calculation; closed circles: experimental data of Girnius (Ref. 6); open circles: experimental data of Nagata [Ref. 5(b)]. The total excitation cross section $Q_{5p_{Rb}}$ (dashed line) is intended to represent all other inelastic processes than $Q_{(2s+2p)_H}$.

charge exchange at keV collision energies.

The unlikeliness of a direct $ns\rightarrow np$ excitation of the alkali atom in the investigated energy range implies that this process is mediated by the H ($n=2$) charge-exchange channel. Such a branching is expected to be enhanced by the smallness of the resonance-energy defect between the H ($n=2$) $+A^+$ and $H^+ + A^*(np)$ channels. This view is indeed supported by the relative behavior of the charge exchange and excitation cross sections for all the H^+-alkali systems. It should be noticed however that the $A^*(np)$ excitation channel and the H ($n=2$) charge-exchange channel [namely the active H (ϕ^+) one] split apart at finite internuclear distances due to long-range charge-dipole interactions (a very similar effect is discussed in some detail in Ref. 15). This effect explains the

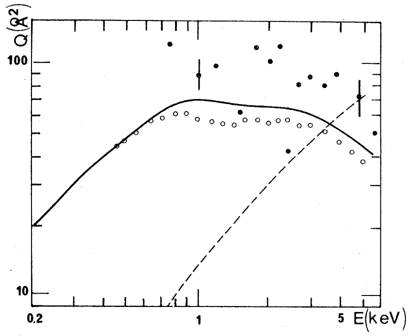

FIG. 7. Total summed $Q_{(2s+2p)_H}$ charge-exchange cross section for the H^+-K collision; full line: present calculation; closed circles: experimental data of Gruebler *et al.* (Ref. 3); open circles: experimental data of Nagata [Ref. 5(b)]. The total excitation cross section Q_{4p_K} (dashed line) is intended to represent all other inelastic processes than $Q_{(2s+2p)_H}$.

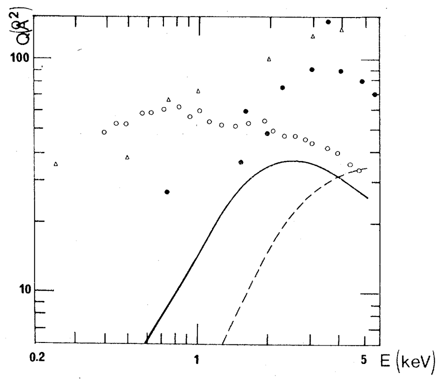

FIG. 8. Total summed $Q_{(2s+2p)_H}$ charge-exchange cross section for the H^+-Na collision; full line: present calculation; closed circles: experimental data of Gruebler *et al.* (Ref. 3); open circles: experimental data of Nagata [Ref. 5(b)]; open triangles: experimental data of McCullough (Ref. 4). The total excitation cross section $Q_{3p_{Na}}$ (dashed line) is intended to represent all other inelastic processes than $Q_{(2s+2p)_H}$.

weakness of the Q_{np_A} cross section at energies where a sizeable charge exchange occurs.

Turning to the charge-exchange results for H^+-Na, Fig. 8 shows that the calculated charge-exchange cross section considerably disagrees with the data of Gruebler *et al.*[3] and McCullough.[4] These authors obtain for H^+-Na as large a total cross section at maximum as in the most resonant H^+-Cs, Rb cases. In view of the behavior of the exchange interaction which hardly matches the resonance-energy defect of reaction (1) for Na the very large cross sections measured by Gruebler *et al.* and McCullough are rather surprising. These data, however, are not confirmed by the recent experiment of Nagata.[5(b)] His measured cross section also plotted in Fig. 8 reduces significantly the gap between theory and experiment above 2 keV. Yet below this energy an important discrepancy still remains. Nevertheless the almost identical cross sections found by Nagata[5(b)] for H^+-K and H^+-Na is most puzzling. It was pointed out by this author[24] that anomalously large charge-exchange cross sections have also been found in other ion-sodium collisions. Since no reasonable alternative collision mechanism can be invoked to explain the present anomaly, we are led to the conclusion that they may have an experimental origin. Because of the mutual agreement between the different experiments for the heavy alkali cases an experimental calibration problem is seemingly ruled out, although accurate absolute calibration is a difficult task to achieve.[3,24] Turning to another possibility, a known difficulty when operating at high temperatures with alkali metals is the presence of dimers in the vapour. Referring to the known molecular properties of Na_2 and Na_2^+ (Ref. 25), the reaction

$$H^+ + Na_2(v \neq 0) \rightarrow H(n=2) + Na_2^+$$

has a smaller resonance-energy defect than reaction (1) for Na which could explain the anomaly. Nevertheless as in "initial growth" or "attenuation" experiments the charge-exchange cross section is derived at low temperatures (low target thickness), the presence of a significant fraction of dimers in the vapour is unlikely. Yet at relatively low temperatures another experimental difficulty arises, namely, the effect of the pollution of the Na vapour by heavier alkali impurities. A 1% potassium impurity in the Na sample can, for a work temperature of 500 °C, be the source of the discussed anomaly. It is our opinion that further experimental endeavour is necessary to solve the H^+-Na charge-exchange problem.

IV. CONCLUSION

The present one-electron PVB model is an efficient procedure to obtain molecular properties and interactions relevant to collision systems involving one active electron. This method has enabled a systematic investigation of the H^+–alkali-atom systems. Charge-exchange excitation in the heavy H^+–Cs, -Rb, and -K systems has been successfully accounted for by our multi state diabatic calculations and is now a well understood problem. On the other hand, the anomaly discussed in the present work for H^+-Na should stimulate further investigations.

ACKNOWLEDGMENTS

The authors would like to thank Dr. R. W. McCullough and Dr. T. Nagata for communicating their data prior to publication and for useful correspondance. Acknowledgments are also due to Dr. J. Pommier and Dr. Vu Ngoc Tuan for useful discussions. The authors are also grateful to Dr. M. Barat and Dr. B. Fastrup for their critical reading of the manuscript.

---

*Also at Centre de Mécanique Ondulatoire Appliquée 23, rue du Maroc, 75 019 Paris, France.

[1] B. L. Donnally, T. Clapp, W. Sauwyer, and M. Schultz, Phys. Rev. Lett. 12, 502 (1964); A. S. Schlachter, P. J. Bjorkholm, D. H. Lyod, L. W. Anderson, and W. Haeberli, Phys. Rev. 177, 184 (1969); G. Spiess, A. Valance, and P. Pradel, Phys. Rev. A 6, 746 (1972); P. Pradel, F. Roussel, A. S. Schlachter, G. Spiess, and A. Valance, *ibid.* 10, 797 (1974); Vu Ngoc Tuan, C. Gautherin, and A. S. Schlachter, *ibid.* 9, 1242 (1974); F. W. Meyer and L. W. Anderson, Phys. Lett. 54A, 733 (1975); F. Brouillard, W. Claeys, and G. Wassenhove, J. Phys. B 10, 687 (1977); F. W. Meyer, C. J. Anderson, and L. W. Anderson, Phys. Rev. A 15, 455 (1977); and G. Van Wasenhove, F. Brouillard, and W. Clayes, in *Abstracts of the Tenth International Conference on the Physics of Electronic and Atomic Collisions*, edited by M. Barat and J. Reinhardt (Commissariat â l'Energie Atomique, Paris, 1977), p. 1264.

[2] P. Pradel, G. Spiess, V. Sidis, and C. Kubach, J. Phys. B 12, 1485 (1979).

[3] W. Gruebler, P. A. Schelzbach, V. Kronig, and P. Marnier, Helv. Phys. Acta 3, 254 (1970).

[4] R. W. McCullough (unpublished).

[5] T. Nagata, J. Phys. Soc. Japan 5, 1622 (1979); T. Nagata, in *Abstracts of the Eleventh International Conference on the Physics of Electronic and Atomic Collisions*, edited by K. Takayanagi and N. Oda (The Society for Atomic Collisional Research, Kyoto, 1979), p. 512.

[6] Girnius, in *Cross Sections for Charge Transfer of Hydrogen Beams in Gases and Vapors in the Energy Range 10 eV-10 keV*, edited by H. Tawara (Research Information Center, IPP/Nagoya University, Nagoya, Japan, 1977).

[7] A. Valance and G. Spiess, J. Chem. Phys. 63, 1487 (1975).

[8] R. E. Olson, E. J. Shipsey, and J. C. Browne, Phys. Rev. A 13, 180 (1976).

[9] V. Sidis and C. Kubach, J. Phys. B 11, 2687 (1978).

[10] (a) A. Valance, Chem. Phys. Lett. 56, 289 (1978); (b) R. E. Olson, R. P. Saxon, and B. Liu, J. Phys. B 13, 297 (1980).

[11] A. Valance, Q. Nguyen-Tuan, and K. Trinh Duc, in *Abstracts of the International Conference on the Physics of Electronic and Atomic Collisions*, edited by K. Takayanagi and N. Oda (The Society for Atomic Collisional Research, Kyoto, 1979), p. 516.

[12] C. Kubach and V. Sidis, Phys. Rev. A 14, 152 (1976).

[13] M. Krauss, P. Maldonado, and A. C. Wahl, J. Chem. Phys. 54, 4944 (1971).

[14] C. E. Moore, *Atomic Energy Levels*, Vol. I, National Bureau of Standards Circ. No. 467 (U.S. GPO, Washington, D. C., 1949).

[15] V. Sidis, C. Kubach, and J. Pommier, Phys. Rev. A 23, 119 (1980).

[16] C. Bottcher, J. Phys. B 11, 507 (1978).

[17] G. A. Hart and P. L. Goodfriend, J. Chem. Phys. 53, 448 (1970).

[18] (a) E. Clementi, D. L. Raimondi, and W. Reinhardt, J. Chem. Phys. 47, 1300 (1967); (b) E. Clementi, IBM J. Res. Dev. 9, 3101 (1965); (c) R. P. Saxon and R. E. Olson, J. Chem. Phys. 67, 2692 (1977).

[19] C. E. Moore, *Atomic Energy Levels*, Vol. II, National Bureau of Standards Circ. No. 467 (U. S. GPO, Washington, D. C., 1952) and Vol. III, National Bureau of Standards Circ. No. 467 (U. S. GPO, Washington, D. C., 1958).

[20] A. Dalgarno and A. E. Kingston, Proc. R. Soc. London 73, 455 (1959).

[21] The ground-state-energy curve correlated with H (1s)

+ A^+ is not considered in the discussion.

[22] M. Barat and W. Lichten, Phys. Rev. A 6, 211 (1972); J. Eichler and U. Willie, *Proceedings of the Tenth International Conference on the Physics of Electronic and Atomic Collisions,* edited by G. Watel (North-Holland, Amsterdam, 1977); C. Falcon, A. Macias, A. Riera, and A. Salin (unpublished).

[23] C. Gaussorgues, R. D. Piacentini, and A. Salin, Comput. Phys. Commun. 10, 223 (1975).

[24] T. Nagata, J. Phys. Soc. Japan 46, 1302 (1979).

[25] J. N. Bardsley, B. R. Junker, and D. W. Norcross, Chem. Phys. Lett. 37, 502 (1976).